Magnetoresistance in the superconducting state at the (111) LaAlO_{3}/SrTiO_{3} interface

S. Davis, Z. Huang, K. Han, Ariando, T. Venkatesan, and V. Chandrasekhar

Phys. Rev. B **96**, 134502 — Published 2 October 2017

DOI: 10.1103/PhysRevB.96.134502

Magnetoresistance in the superconducting state at the (111) $LaAlO_3/SrTiO_3$ interface

S. Davis,[1,*] Z. Huang,[2,3] K. Han,[2,3] Ariando,[2,3,4] T. Venkatesan,[4,5,6] and V. Chandrasekhar[1,†]

[1]*Graduate Program in Applied Physics and Department of Physics and Astronomy, Northwestern University, 2145 Sheridan Road, Evanston, IL 60208, USA*

[2]*NUSNNI-Nanocore, National University of Singapore 117411, Singapore*

[3]*Department of Physics, National University of Singapore 117551, Singapore*

[4]*NUS Graduate School for Integrative Sciences & Engineering, National University of Singapore 117456, Singapore*

[5]*Department of Electrical and Computer Engineering, National University of Singapore 117576, Singapore*

[6]*Department of Material Science and Engineering, National University of Singapore 117575, Singapore*

Condensed matter systems that simultaneously exhibit superconductivity and ferromagnetism are rare due the antagonistic relationship between conventional spin-singlet superconductivity and ferromagnetic order. In materials in which superconductivity and magnetic order is known to coexist (such as some heavy-fermion materials), the superconductivity is thought to be of an unconventional nature. Recently, the conducting gas that lives at the interface between the perovskite band insulators $LaAlO_3$ (LAO) and $SrTiO_3$ (STO) has also been shown to host both superconductivity and magnetism. Most previous research has focused on LAO/STO samples in which the interface is in the (001) crystal plane. Relatively little work has focused on the (111) crystal orientation, which has hexagonal symmetry at the interface, and has been predicted to have potentially interesting topological properties, including unconventional superconducting pairing states. Here we report measurements of the magnetoresistance of (111) LAO/STO heterostructures at temperatures at which they are also superconducting. As with the (001) structures, the magnetoresistance is hysteretic, indicating the coexistence of magnetism and superconductivity, but in addition, we find that this magnetoresistance is anisotropic. Such an anisotropic response is completely unexpected in the superconducting state, and suggests that (111) LAO/STO heterostructures may support unconventional superconductivity.

Ferromagnetism is traditionally considered antithetical to conventional superconductivity: electron spin moments are aligned in a ferromagnet, while conventional s-wave superconductivity requires the anti-alignment of the spin moments of the two electrons in a Cooper pair. While there do exist systems in which superconductivity and magnetism coexist, the pairing in these systems is thought to be of an unconventional nature: examples are heavy-fermion materials like UGe_2 and UPt_3 that are thought to have p or f-wave orbital pairing in triplet spin states in some phases.[1,2] More recently, ferromagnetism and superconductivity have been found to coexist at the LAO/STO interface.[3–6] Low temperature magnetotransport measurements show that the influence of the ferromagnetism on the superconducting state at the LAO/STO occurs primarily through the external magnetic field arising from the ferromagnet,[7] although the observation of anisotropic magnetoresistance (AMR) suggests that there is direct exchange coupling between the charge carriers and the magnetic moments at the interface.[8–10].

Most experiments on LAO/STO interfaces have been performed on samples where the interface is in the (001) crystal plane.[3–8] In the past few years, interest has grown in LAO/STO interfaces in the (111) crystal orientation. The Ti atoms at the (111) LAO/STO interface have hexagonal symmetry,[11,12] and consequently have been predicted to have potential topological properties,[13] and to possibly host time-reversal symmetry breaking superconducting pairing states.[14] Electrical transport measurements on the conducting carrier gas at the (111) LAO/STO interface have found not only a superconducting state[15–17] but also the presence of strong anisotropy in almost all properties when measured along different surface crystal directions, including longitudinal resistance, Hall effect, quantum capacitance, AMR and superconductivity.[17–20] Here we show that the magnetoresistance at or in the superconducting state is hysteretic and also anisotropic. As with the (001) LAO/STO devices, the presence of a hysteretic magnetoresistance (MR) in the (111) LAO/STO devices indicates magnetism coexisting with superconductivity.[3,7] The anisotropic nature of the MR reinforces observation of the anisotropic superconducting properties seen previously, and raises the possibility that the superconducting state may be unconventional in nature.

The samples in this study consisted of four Hall bar devices fabricated on a single substrate, such that two 600 μm long by 100 μm wide Hall bars lie along the $[1\bar{1}0]$ direction and two lie along the $[\bar{1}\bar{1}2]$ surface crystal direction of the (111) LAO/STO interface. Details about the film synthesis and sample fabrication can be found in earlier publications.[18,19] The properties of the devices depend on post-growth treatment. Three differ-

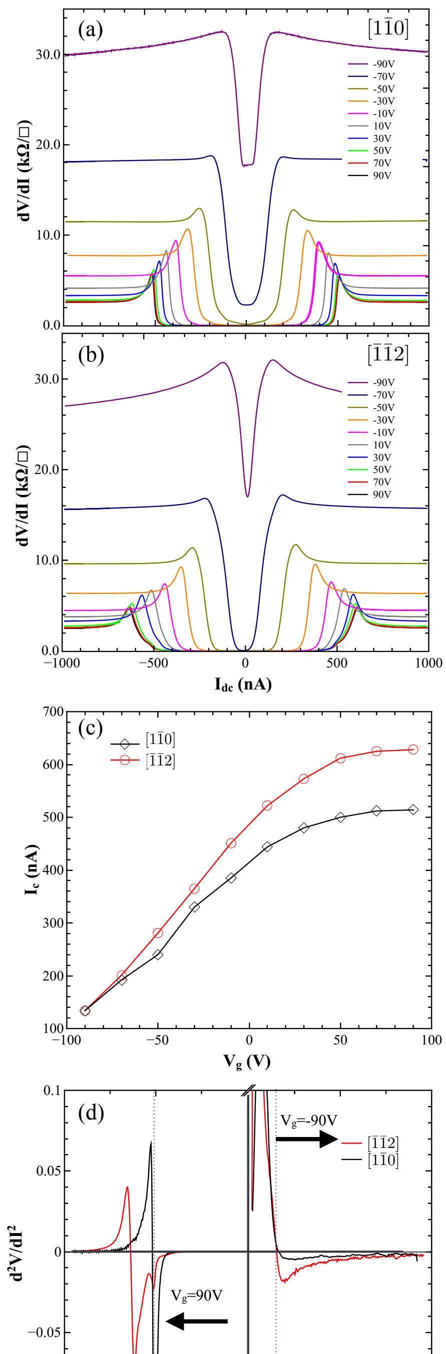

FIG. 1. Longitudinal differential resistance dV/dI vs dc current I_{dc} at 30 mK at different gate voltages V_g for Hall bars aligned along the $[1\bar{1}0]$ crystal direction (a) and the $[\bar{1}\bar{1}2]$ crystal direction (b). (c) Critical current I_c for the two directions as a function of V_g. (d) Second derivative d^2V/dI^2 vs. I_{dc} along the two crystal directions for V_g=90 V (negative x axis) and V_g=-90 V (positive x axis).

ent post-growth treatments were discussed in an earlier publication:[19] annealing in a O_2 environment, annealing in a Ar/H_2 environment, and ultraviolet (UV) irradiation under ambient conditions. It is only for the Ar/H_2 annealed samples that the devices show a zero resistance state along both surface crystal directions, and hence we discuss here only these devices.[17] We note, however, that while the Ar/H_2 annealed samples had a larger concentration of oxygen vacancies, these oxygen vacancies are not directly the diving factor of the superconductivity in the system. Instead, based on studies in (001) LAO/STO,[3,7] superconductivity depends on the carrier concentration, which can be varied with a back gate voltage or other means (in this case, by varying the oxygen carrier concentration); we believe the situation for (111) LAO/STO is similar. Additionally, the Ar/H_2 annealed samples have a far lower sheet resistance and show far less anisotropy than either as-grown samples or samples subjected to a O_2 anneal or UV irradiation;[19] nevertheless, as we show below, the anisotropy is quite evident. The Hall bars were measured in an Oxford Kelvinox MX100 dilution refrigerator using conventional lock-in techniques. Both sets of devices on the showed quantitatively similar behavior; here we only report the results for two devices on which we performed the most extensive measurements. The other two Hall bar devices have quantitatively and qualitatively similar behavior and other Ar/H_2 samples show similar behavior.

Figures 1(a) and (b) show the differential resistance dV/dI as a function of dc current I_{dc} at 30 mK for two Hall bars, one aligned along the $[1\bar{1}0]$ direction, and one along the $[\bar{1}\bar{1}2]$ direction, for various values of the back gate voltage V_g. The devices were cooled from 4 K with a gate voltage $V_g = -10$ V applied. As can be seen, both devices are superconducting for positive gate voltages, leaving the zero resistance state for large negative V_g ($V_g \sim -50$V for the $[1\bar{1}0]$ Hall bar, and $V_g \sim -70$V for the $[\bar{1}\bar{1}2]$ Hall bar). However, both Hall bars show a decrease in resistance near zero bias even at the largest negative $V_g = -90$ V, indicating the presence of superconducting correlations. It is clear from these traces that the superconducting characteristics are anisotropic, even in these Ar/H_2 annealed samples which show much less anisotropy than O_2 annealed or UV irradiated devices.[19] The anisotropy is visible in the critical current I_c (defined as the current I_{dc} at which the maxima in dV/dI occur in Figs. 1(a) and (b)) as a function of V_g for both Hall bars, which is shown in Fig. 1(c). While I_c is the same for both directions at large negative V_g, I_c becomes progressively larger for the $[\bar{1}\bar{1}2]$ Hall bar in comparison to the $[1\bar{1}0]$ Hall bar as V_g is increased above -50 V. Surprisingly, the superconducting transitions from the zero resistance state with increasing $|I_{dc}|$ are sharper for the $[1\bar{1}0]$ direction than for the $[\bar{1}\bar{1}2]$ direction for positive V_g, even though the $[1\bar{1}0]$ direction has higher normal state resistance at all gate voltages. Closer inspection of the

dV/dI vs. I_{dc} traces for the $[\bar{1}\bar{1}2]$ Hall bar show that for large positive values of V_g, a small peak appears at a value of I_{dc} corresponding to I_c in the $[1\bar{1}0]$ direction. This is more clearly seen by examining the second derivative d^2V/dI^2 vs. I_{dc}, shown in Figure 1(d) for V_g=-90 and V_g=90 V. d^2V/dI^2 is zero when dV/dI is maximum, and hence the zero crossings of d^2V/dI^2 determine I_c. For V_g=-90 V, d^2V/dI^2 crosses zero at approximately the same current for both crystal directions, and hence the I_c's are also approximately the same. For V_g=90 V, the zero crossings for the two crystal directions are quite different, corresponding to the different I_c's seen in Fig. 1(c). However, d^2V/dI^2 vs I_{dc} for the $[\bar{1}\bar{1}2]$ direction shows a dip near the critical current for the $[1\bar{1}0]$ direction, a signature of the small peak in the $[\bar{1}\bar{1}2]$ dV/dI traces mentioned above. This suggests that measurements along the $[\bar{1}\bar{1}2]$ Hall bar for positive V_g also sample the superconducting characteristics along the $[1\bar{1}0]$ direction, although the reverse is apparently not true. This may be the reason behind the broader transitions in the $[\bar{1}\bar{1}2]$ Hall bar for large positive V_g.

The difference between the two crystal directions is also reflected in the temperature-dependent superconducting transition, shown in Fig. 2(a). The transition in the $[\bar{1}\bar{1}2]$ direction is broader, although the zero-resistance state is reached at the same temperature in both directions. One can also obtain the Ginzburg-Landau superconducting coherence length ξ_S and the thickness d of the conducting gas by measuring the phase diagram (superconducting transition temperature T_c as a function of magnetic field) in parallel and perpendicular magnetic fields.[3,7] In a perpendicular field, the critical field $H_{c\perp}$ is roughly the field required to put one superconducting flux quantum $\Phi_0 = h/2e$ in an area the size of ξ_S^2,[21]

$$H_{c\perp} = \frac{\Phi_0}{2\pi\xi_S^2(T)} \quad (1)$$

where the temperature dependent superconducting phase coherence length is given by

$$\xi_S(T) = \alpha\frac{\xi_0}{\sqrt{(1-T/T_c)}}. \quad (2)$$

Here ξ_0 is the zero temperature coherence length, and α=0.74 or 0.86 for the clean and dirty limit respectively.[21] The dependence of $H_{c\perp}$ on T is therefore linear, with a slope given by

$$\frac{dH_{c\perp}}{dT} = -\frac{\Phi_0}{2\pi\xi_0^2 T_c}, \quad (3)$$

where we have taken $\alpha \sim 1$. Thus by measuring the slope of the phase diagram and T_c, one can determine ξ_0. In a parallel field, for a superconductor whose thickness d is less than ξ_S, the area is restricted by d, hence the parallel critical field is given by[21]

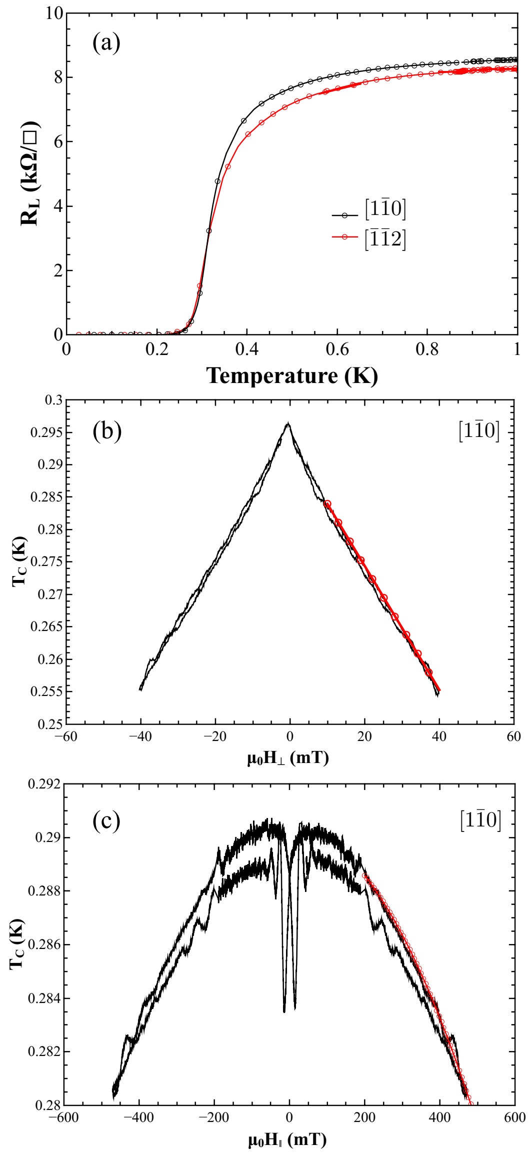

FIG. 2. (a) Sheet resistance as a function of temperature for the $[1\bar{1}0]$ and $[\bar{1}\bar{1}2]$ Hall bars, with V_g=-10 V. (b) Superconducting transition temperature T_c as a function of perpendicular magnetic field for the $[1\bar{1}0]$ Hall bar for V_g=100 V. The line with symbols is a fit to the linear dependence.(c) T_c as function of parallel magnetic field for the $[1\bar{1}0]$ Hall bar for V_g=100 V. The line with symbols is a fit to a quadratic dependence.

$$H_{c\parallel} = \frac{\sqrt{3}\Phi_0}{\pi\xi_S(T)d}, \quad (4)$$

so that $T_c(H)$ should have a quadratic dependence on H. Fitting this dependence, using the value of ξ_0 obtained from the perpendicular field phase diagram, one can obtain an estimate for the thickness d of the superconductor.

Figures 2(b) and (c) show the phase diagrams for the Hall bar oriented along the $[1\bar{1}0]$ crystal directions in magnetic fields perpendicular and parallel to the interface, for V_g=100 V (results along the $[\bar{1}\bar{1}2]$ direction are similar). These data were taken by maintaining the resistance of the device at the midpoint of the resistive superconducting transition while continuously sweeping the magnetic field. Each of these traces took approximately 20 hours to complete. As expected, the slope of T_c vs $H_\perp$ is linear, and from the slope, we obtain a zero temperature coherence length of ξ_0= 26 nm. The phase diagram in parallel field is more complicated: while the overall background is quadratic as expected, near zero field, we observe hysteresis in the field dependence, with sharp dips in T_c near zero field. This hysteresis is a result of the hysteresis in the MR, which is discussed in detail below, and is similar to what is observed in (001) LAO/STO devices.[3,7] Fitting the data for $|\mu_0 H_\parallel| > 50$ mT to the expected quadratic form, we obtain a superconducting film thickness of $d \sim$7 nm. This value is for V_g=100 V, where the conducting gas thickness is expected to be maximum, so that the film thickness at other gate voltages will be smaller. We note that this value is smaller than the values typically reported in (001) LAO/STO, which usually are of order 10-15 nm.[3,7,15]

We now discuss the MR along the two crystal directions in a magnetic field perpendicular to the interface well below the superconducting transition. Figure 3(a) shows the MR along the two crystal directions for V_g=-30 V at 30 mK. The traces for both directions are hysteretic, similar to what has been observed earlier for (001) LAO/STO devices, showing the coexistence of magnetism and superconductivity in (111) LAO/STO devices.[3,7] While the MR traces along the two directions appear very similar at this gate voltage, the differences are accentuated as V_g is decreased. Figs. 3(b) and (c) show the perpendicular MR for different gate voltages along the $[1\bar{1}0]$ and $[\bar{1}\bar{1}2]$ crystal directions respectively. Since the normal state resistance R_N changes by an order of magnitude over the gate voltage range, the resistance values for each gate voltage are normalized by R_N, which we take to be the value of dV/dI at $I_{dc} = 2.5$ μA at 30 mK for that value of V_g (Figs. 1(a) and (b)).

Consider first the features of the MR that are similar to those observed in (001) LAO/STO devices. The change in resistance with magnetic field is large, a significant fraction of R_N, particularly at negative V_g. This appears similar to the (001) LAO/STO devices, where a large MR was observed in the superconducting state.[7] On sweeping from negative to positive magnetic field, a peak is observed in the MR at ~34 mT, which grows in relative magnitude as V_g is decreased. A mirror symmetric peak is observed at ~-34 mT on sweeping down in magnetic field. Similar hysteretic peaks in the MR at small fields have been observed in the (001) LAO/STO devices,[3,7] and have been associated with the magnetization dynamics of the ferromagnet at the interface: it is reasonable to assume that the origin of the peaks here is

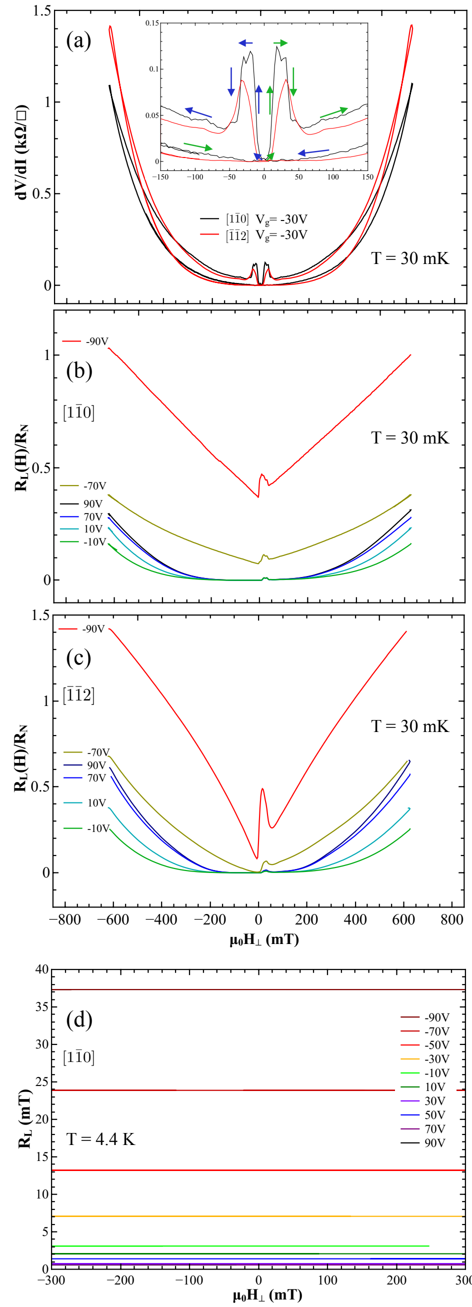

FIG. 3. (a) Magnetoresistance (MR) of the $[\bar{1}\bar{1}2]$ and $[1\bar{1}0]$ Hall bars at 30 mK, at a back gate voltage of V_g=-30 V. Inset:Expanded plot of the MR near zero field, showing the hysteresis in magnetic field. (b), (c) Normalized MR for the $[1\bar{1}0]$ (b) and $[\bar{1}\bar{1}2]$ (c) crystal directions, at 30 mK, for various gate voltages. For clarity, only the sweeps from negative to positive magnetic field are shown. (d) longitudinal MR along the $[1\bar{1}0]$ direction at 4.4 K.

similar. In contrast, at 4 K, there is almost no MR: Fig. 3(d) shows the MR along the $[1\bar{1}0]$ direction for various gate voltages at 4 K. The curves are flat to within our noise (MR for the $[\bar{1}\bar{1}2]$ direction is similarly flat).

There are, however, some important differences between the (001) and (111) LAO/STO samples. First, in the (001) LAO/STO devices, once a perpendicular magnetic field was applied, the samples never returned to a true zero resistance state unless they were warmed up well above the superconducting transition.[7] This is consistent with the expected vortex dynamics in a two-dimensional superconductor. In contrast, for positive values of V_g, the resistance of the (111) LAO/STO devices vanishes as the magnetic field is swept to zero, as can be seen from Figs. 3(b) and (c). Second, for larger perpendicular magnetic fields ($\geq$ 150 mT), the MR in (001) LAO/STO devices for positive V_g (*i.e.*, in the superconducting regime) became non-hysteretic and saturated at a value corresponding to R_N. As can be seen from Figs. 3(b) and (c), the MR for the (111) devices gives no indication of saturating even over much larger field scales for either crystal direction: indeed, with R_N defined as above, the resistance exceeds R_N for magnetic fields greater than 600 mT in both crystal directions for $V_g = -90$ V. Third, while the general shapes of the MR curves in perpendicular magnetic field B in the (001) LAO/STO devices were similar in shape and curvature, changing primarily in magnitude as V_g changed, the shapes of the MR curves for the (111) devices change significantly over the gate voltage range measured. For positive V_g, the MR is quadratic in B, with positive curvature for $B > 50$ mT, similar to what was observed in the (001) devices. For large negative V_g, however, the curvature gradually changes; for $V_g = -90$ V, the MR for the $[1\bar{1}0]$ direction is strikingly linear, while the curvature of the MR trace for the $[\bar{1}\bar{1}2]$ direction becomes negative. It is also in this gate voltage regime that the resistance at the largest fields exceeds R_N. MR that is quasi-linear in B has been reported recently in a number of materials with potential topological properties, where it has been suggested that it might be associated with Dirac bands in the lowest Landau level.[22] The difference in our samples is that the large, quasi-linear MR is observed only at very low temperatures (it disappears at 4 K), and the quasi-linear behavior persists down to very small magnetic fields. Its appearance at low temperatures suggests it might be associated with superconductivity; on the other hand, the fact that the resistance in this gate voltage regime at even moderate magnetic fields exceeds R_N indicates that its origin may be associated with normal magnetotransport that only manifests itself at the lowest temperatures.

A fourth distinct difference between the (001) and (111) LAO/STO devices is that the MR in the (111) LAO/STO devices is different along different crystal directions, reflecting the anisotropy found in almost all the other properties. As with those other properties, this anisotropy in the MR is most evident for negative V_g, as can be seen by comparing the MR curves for $V_g = -90$ V for the two crystal directions where the resistivity is higher.

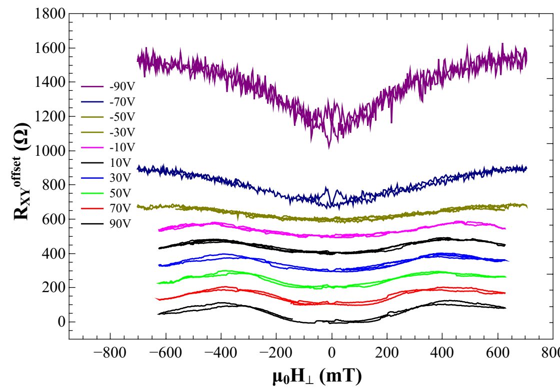

FIG. 4. Hall magnetoresistance for the $[1\bar{1}0]$ direction at 30 mK for a range of V_g. For clarity each of the curves is offset from the next gate voltage by 100 Ω.

One final difference between the (001) and (111) LAO/STO devices is seen in the Hall response in the superconducting state. Figure 4 shows the transverse (Hall) resistance of the $[1\bar{1}0]$ Hall bar for various gate voltages V_g as a function of magnetic field at 30 mK. The Hall resistance appears to be symmetric in magnetic field; in fact, there is a small antisymmetric component whose slope is approximately 1/3 of the Hall slope at 4.4 K ($\sim$ 35 Ω/T). In general, a symmetric component to the transverse resistance may appear due to a small misalignment of the transverse voltage probes, which results in a fraction of the longitudinal MR appearing in the Hall measurement. In our case, the misalignment is ~ 1 μm over a total length between longitudinal voltage probes of 600 μm ($\sim$0.2%). At V_g=-90 V, with this level of misalignment, we might expect to see a symmetric signal of order $\sim$ 180 Ω in the transverse Hall signal coming from the longitudinal MR, while the overall resistance change is $\sim$ 400 Ω. However, this cannot be the origin of the entire transverse MR, since the shape of the transverse MR curves do not reflect the corresponding longitudinal resistance curves, as can be seen by comparing Figs. 3(b) and 4. This is evident in all the traces, particularly the ones at large V_g, where the longitudinal resistance vanishes over a range of magnetic fields, and hence there should be no contribution from misaligned contacts. It is known that the motion of vortices in superconductors can give rise to a symmetric transverse voltage, and we believe that the remaining contribution to the Hall signal is due to vortex dynamics under the influence of magnetic field and measurement current.[23,24] Another possible source of this symmetric Hall signal could be the tetragonal domains that have been widely reported in

(001) LAO/STO heterostructures.[25,26] Scanning SQUID measurements have shown that current flow is enhanced along the boundaries of such domains,[26] which could produce a symmetric component that is larger than expected from the mismatch of the transverse voltage probes. We also note that these data are quite different from the transverse MR observed in the superconducting state in (001) LAO/STO samples.[3] In that case, the transverse MR is hysteretic, as it is for large negative V_g here, but the linear antisymmetric component of the transverse MR is large and comparable to its value at temperatures well above the superconducting transition.

In conclusion, we have shown that the (111) LAO/STO interface exhibits the coexistence of ferromagnetic and superconducting phases; similar to the (001) interface this coexistence is seen most prominently in hysteretic MR. Additionally we also observe that the T_c vs $H_{\perp/\parallel}$ phase diagram is strongly hysteretic, giving further evidence of coexistence; furthermore, using these curves we have determined the thickness of the gas and ξ_0 are of the same order, albeit slightly smaller, than those seen in (001) LAO/STO. However, standing in stark difference to the behavior at the (001) interface, the (111) interface shows a return to a zero resistance state at low field, larger high field hysteresis, and a superconducting Hall effect that is three orders of magnitude larger than in the (001) interfaces. These differences may originate from the more disordered nature of the gas at the (111) interface, corroborated by the higher normal state resistances, or possibly from a exotic source such as different Rashba coupling the two in-plane crystal directions.[27] More importantly the (111) interface shows strong anisotropy that is not observed in (001) interface, which shows up in the differential resistance vs I_{dc} and also the hysteretic MR. This coupling opens a new avenue to investigate possibly unconventional two dimensional superconductivity, and will require further work to elucidate its origin.

ACKNOWLEDGMENTS

Work at Northwestern was funded through a grant from the U.S. Department of Energy through Grant No. DE-FG02-06ER46346. Work at NUS was supported by the MOE Tier 1 (Grant No. R-144-000-364-112 and R-144-000-346-112) and Singapore National Research Foundation (NRF) under the Competitive Research Programs (CRP Award Nos. NRF-CRP8-2011-06, NRF-CRP10-2012-02, and NRF-CRP15-2015-01).

---

* samueldavis2016@u.northwestern.edu
† v-chandrasekhar@northwestern.edu

[1] H. Kotegawa, S. Kawasaki, A. Harada, Y. Kawasaki, K. Okamoto, G-q Zheng, Y. Kitaoka, E. Yamamoto, Y. Haga, Y. Onuki, K. M. Itoh, and E.E. Haller, *J. Phys. Cond. Mat.* **15**, S2043-S2046 (2003).
[2] W. J. Gannon, W. P. Halperin, C. Rastovski, K. J. Schlesinger, J. Hlevyack, M. R. Eskildsen, A. B. Vorontsov, J. Gavilano, U. Gasser, and G. Nagy, *NJP* **17**, (2015).
[3] D. A. Dikin, M. Mehta, C. W. Bark, C. M. Folkman, C. B. Eom, and V. Chandrasekhar, *Phys. Rev. Lett.* **107**, 056802 (2011).
[4] T. Schneider, A. D. Caviglia, S. Gariglio, N. Reyren, and J.-M. Triscone, *Phys. Rev. B* **79**, 184502 (2009).
[5] L. Li, C. Richter, J. Mannhart, and R.C. Ashoori, *Nat. Phys.* **7**, 762 (2011).
[6] J. A. Bert, B. Kalisky, C. Bell, M. Kim, Y. Hikita, H. Y. Hwang & K. A. Moler, *Nat. Phys.* **7**, 767 (2011).
[7] M.M. Mehta, D.A. Dikin, C.W. Bark, S. Ryu, C.M. Folkman, C.B. Eom & V. Chandrasekhar, *Nat.Commun.* **3** 1959 (2012).
[8] A. Joshua, J. Ruhman, S. Pecker, E. Altman, and S. Ilani, *PNAS* **110**(24), 9633-9638 (2013).
[9] L. Miao, R. Du, Y. Yin, and Q. Li, *Appl. Phys. Lett.* **109**, 261604 (2016).
[10] A. Annadi, Z. Huang, K. Gopinadhan, X. Renshaw Wang, A. Srivastava, Z. Q. Liu, H. Harsan Ma, T. P. Sarkar, T. Venkatesan, and Ariando, *Phys. Rev. B* **874**, 201102 (2013).
[11] T.C. Rodel, C. Bareille, F. Fortuna, C. Baumier, F. Bertran, P. Le Fevre, M. Gabay, O. Hijano Cubelos, M. J. Rozenberg, T. Maroutian, P. Lecoeur, & A. F. Santander-Syro, *Phys. Rev. Applied* **1**, 051002 (2014).
[12] S. McKeown-Walker, A. de la Torre, F. Y. Bruno, A. Tamai, T.K. Kim, M. Hoesch, M. Shi, M. S. Bahramy, P. D. C. King, and F. Baumberger, *Phys.Rev.Lett.* **113**, 177601 (2014).
[13] D. Doennig, W. E. Pickett and Rossitza Pentcheva, *Phys.Rev.Lett.* **111**, 126804 (2013).
[14] M. S. Scheurer, D. F. Agterberg, and J. Schmalian, *NPJ: Quantum Materials* **2**:9, (2017).
[15] A.M.R.V.L. Monteiro, D.J. Groenendijk, I. Groen, J. de Bruijckere, R. Gaudenzi, H.S.J. van der Zant, and A.D. Caviglia,*Phys. Rev. B* **96**, 020504(R) (2017).
[16] P.K. Rout, E. Maniv, and Y. Dagan, **arXiv:**1706.01717V1 (2017).
[17] S. K. Davis, Z. Huang, K. Han, Ariando, T. Venkatesan, V. Chandrasekhar, **arXiv:**1704.01203 (2017).
[18] S. K. Davis, Z. Huang, K. Han, Ariando, T. Venkatesan, V. Chandrasekhar, *Phys. Rev. B* **95**, 035127 (2017).
[19] S. K. Davis, Z. Huang, K. Han, Ariando, T. Venkatesan, V. Chandrasekhar, *Adv. Mater. Interfaces* **1600830**, (2017).
[20] P. K. Rout, I. Agireen, E. Maniv, M. Goldstein, and Y. Dagan1, **Phys. Rev. B** *95*, 241107(R) (2017).
[21] M. Tinkham, *Introduction to Superconductivity* (McGraw-Hill Inc., New York, 1996), 2^{nd} edition, p119.
[22] X. Wang, Y. Du, S. Dou, and C. Zhang, *Phys. Rev. Lett.* **108**, 266806 (2012).
[23] N. B. Kopnin and A. V. Lopatin, *Phys. Rev. B* **52**, 21 (1995).

[24] N. B. Kopnin, B. I. Ivlev, and V. A. Kalatsky, *J. Low Temp. Phys.* **90**, 1 (1993).

[25] H. J. Harsan Ma, S. Scharinger, S. W. Zeng, D. Kohlberger, M. Lange, A. Stohr, X. Renshaw Wang, T. Venkatesan, R. Kleiner, J. F. Scott, J. M. D. Coey, D. Koelle, and Ariando *et al.*, *Phys. Rev. Lett.* **116**, 257601 (2016).

[26] B. Kalisky, E. M. Spanton, H. Noad, J. Kirtley, K. C. Nowack, C. Bell, H. K. Sato, M. Hosoda, Y. Xie, Y.Hikita, C. Woltmann, G. Pfanzelt, R. Jany, C. Richter, H. Y. Hwang, J. Mannhart & K. A. Moler, *Nature Materials* **12**, 1091-1095 (2013).

[27] K. Gopinadhan, A. Annadi, Y. Kim, A. Srivastava, B. Kumar, J. Chen, J. M. D. Coey, Ariando, & T. Venkatesan, *Adv. Electron. Mater.* **1**, 1500114 (2015).